Unique progressive cleavage mechanism of HIV reverse transcriptase RNase H

Michele Wisniewski*, Mini Balakrishnan*, C. Palaniappan*†, Philip J. Fay*, and Robert A. Bambara*‡§

*Department of Biochemistry and Biophysics, and ‡Cancer Center, University of Rochester, Rochester, NY 14642

Communicated by Fred Sherman, University of Rochester School of Medicine and Dentistry, Rochester, NY, August 16, 2000 (received for review June 26, 2000)

HIV-1 reverse transcriptase (RT) degrades the plus strand viral RNA genome while synthesizing the minus strand of DNA. Many RNA fragments, including the polypurine tracts, remain annealed to the new DNA. Several RTs are believed to bind after synthesis to degrade all RNA fragments except the polypurine tracts by a polymerization-independent mode of RNase H activity. For this latter process, we found that RT positions the RNase H active site approximately 18 nt from the 5′ end of the RNA, making the primary cut. The enzyme rebinds or slides toward the 5′ end of the RNA to make a secondary cut creating two products 8–9 nt long. RT then binds the new 5′ end of the RNA created by the first primary or the secondary cuts to make the next primary cut. In addition, we observed another type of RNase H cleavage specificity. RT aligns the RNase H active site to the 3′ end of the RNA, cutting 5 residues in. We determined the relative rates of these cuts, defining their temporal order. Results show that the first primary cut is fastest, and the secondary and 5-nt cuts occur next at similar rates. The second primary cuts appear last. Based on these results, we present a model by which RT progressively cleaves RNA fragments.

HIV is the causative agent of AIDS (1). To establish an infection, HIV must integrate a double-stranded viral DNA into the host chromosome (2). The virus-encoded reverse transcriptase (RT) converts the single-stranded viral RNA genome into that double-stranded DNA. RT uses several different catalytic activities in this process. The polymerase function catalyzes DNA synthesis on RNA and DNA templates (3). RT also has an RNase H active site that cleaves RNA when annealed to DNA. RNase H activity is required for a number of steps in viral replication, including formation of primers and primer strand transfers (4). An important role for the RNase H is the complete removal of the original genomic RNA during the synthesis of the double-stranded DNA (5, 6).

The genomic viral RNA first is converted to an RNA/DNA hybrid and then to double-stranded DNA. Synthesis of the second DNA strand necessitates complete removal of the original RNA (7, 8). The RNA genome is cut into small segments during and after synthesis of the RNA/DNA hybrid (9–11). Studies show that two different modes of RNase H activity are important for the removal of the RNA (5, 12, 13). The first mode is carried out by the same RT performing DNA synthesis. This is the polymerization-dependent mode of cleavage (9–11, 14–17). We showed that the HIV-1 RT synthesizing DNA leaves RNA oligomers in its wake, many still bound to the extended DNA primer (17, 18). These residual RNAs occur because cleavages of the RNA template happen less frequently than nucleotide addition. Kati *et al.* (19) examined the rates of both catalytic activities of RT and found that the polymerization rate is 7–10 times faster than the RNase H rate. This result demonstrates that the two activities are uncoupled, such that several nucleotides are added in the time required for each RNase H-directed cleavage. RT leaves RNA fragments still bound to the DNA template. Because a virion contains 50–100 copies of RT and two RNA genomes, we believe that free RTs will bind and cleave the remaining RNA fragments by a polymerase-independent mode of cleavage (7, 13–15, 20, 21).

Another possibility for the removal of the residual RNAs is that RT could displace them during DNA synthesis. Recently, a study using murine leukemia virus RT showed that the wild-type enzyme supports a greater amount of synthesis on a DNA template with an annealed downstream RNA than the RNase H-minus mutant (22). This result indicates that the RT with RNase H activity has a higher efficiency for the removal of downstream RNA. Furthermore, Fuentes *et al.* (8) show by using similar substrates that RT has higher affinity for the RNA fragments versus the DNA primer. In enzyme excess, RT cleaved the majority of the RNA before it interfered with primer elongation. This result indicates that RNA fragments are degraded effectively before plus-strand synthesis. Overall, both studies support further that RT preferentially removes residual RNAs by the polymerase-independent mode of cleavage.

We have previously described basic features of this mode of cleavage (20, 21). Our studies have shown RT to align the polymerase active site near the 5′ end of the RNA (Fig. 1). This mode of binding places the RNase H active site 16–19 nt downstream on the RNA, where a primary cut is made (20). The length of the product of this cleavage corresponds to the distance between the polymerase and RNase H active sites as shown by crystallographic, biochemical, and footprinting data (23–27). RT also can move or position the polymerase active site further 3′ on the DNA template to place the RNase H site 8–9 nt from the 5′ end of the RNA to create the secondary cut. Because the residual RNAs vary in length, longer RNAs would require several additional cleavage events for complete removal. In this study, we examine RNase H activity on two RNA fragments of different lengths and determine the positions of the cuts that remove the fragments. We also determine the rates of each type of cut, which indicate the order of events in the cleavage process. Based on these measurements and interpretations, we propose a comprehensive model of the cleavage mechanism.

Materials and Methods

Materials. The DNA template was purchased from Integrated DNA Technologies (Coralville, IA). RNA oligomers were prepared from the Ambion (Austin, TX) T7-MEGAshortscript kit. The RNA was quantified by a Ribogreen assay supplied by Molecular Probes. Purified HIV reverse transcriptase was generously provided by Genetics Institute (Cambridge, MA). *Acc*I, the Klenow fragment, and T4 kinase were purchased from Roche Molecular Biochemicals. The *Nla*III and T4 RNA ligase

Abbreviation: RT, reverse transcriptase.

†Present address: 800 Centennial Avenue, Piscataway, NY 08855.

§To whom reprint requests should be addressed at: University of Rochester, 601 Elmwood Avenue, Box 712, Rochester, NY 14642. E-mail: robert_bambara@urmc.rochester.edu.

The publication costs of this article were defrayed in part by page charge payment. This article must therefore be hereby marked "*advertisement*" in accordance with 18 U.S.C. §1734 solely to indicate this fact.

Article published online before print: *Proc. Natl. Acad. Sci. USA*, 10.1073/pnas.210392297. Article and publication date are at www.pnas.org/cgi/doi/10.1073/pnas.210392297

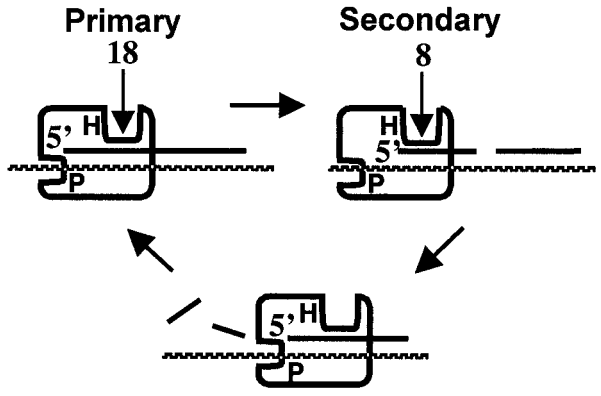

Fig. 1. A stepwise mechanism of HIV RT RNase H. Pattern lines represent DNA, whereas the solid lines represent RNA. The rectangle represents RT with the indents corresponding to the polymerase (P) and the RNase H (H) active sites. The numbered arrows indicate the length of cleavage products. The same symbols are used in the following figures. The schematic shows a linear order of cleavage events: primary, secondary, next primary, then next secondary.

were from New England Biolabs. All reactions were performed by using conditions specified by the manufacturers.

Transcription *in Vitro*. The pBSM13+ plasmid was linearized by *Acc*I or *Nla*III and added to a transcription reaction *in vitro* (Ambion T7-MEGAshortscript kit) creating the 41- and 50-nt RNA transcripts.

5′ End Labeling of the RNA. The 41- and 50-nt RNAs were labeled at the 5′ ends with 6,000 Ci (222 TBq)/mmol[γ-^{32}P]ATP (1 Ci = 37 GBq) by using T4 kinase. Excess radionucleotides were removed by using a Tris RNase-free P30 Micro Bio-Spin column from Bio-Rad. The RNA was PAGE-purified and eluted overnight with 500 μl of a buffer containing 0.1% SDS, 1 mM EDTA, and 0.5 M ammonium acetate. Both RNAs were ethanol-precipitated and resuspended in 10 mM Tris·HCl and 1 mM EDTA buffer, pH 8.0.

3′ End Labeling of the RNA. The RNA was 3′ end labeled by using two different methods, with similar results. In one, RNA was extended by one [α-^{32}P]dATP by using the Klenow fragment. Alternatively, RNA was added to a mixture of α-P32 pCp, T4 RNA ligase, 10% DMSO, and manufacturer's supplied buffer. This reaction was incubated at 15°C for 14 h. RNA from both methods was purified as described above.

Hybridization. The 41- and 50-nt RNAs both were annealed to a 77-nt DNA template. The sequences of the substrates are: 77-nt DNA, 5′-TGCATGCCTGCAGGTCGACTCTAGAGGATC-CCCGGGGTACCGAGCTCGAATTCGCCCTATAGTGA-GTCGTATTACAAT-3-′; 41-nt RNA, 5′-GGGCGAAUUCGA-GCUCGGUACCCGGGGAUCCUCUAGAGTCG-3-′; and 50-nt RNA, 5′-GGGCGAAUUCGAGCUCGGUACCCGGG-GAUCCUCUAGAGTCGACCUGCAGG-3-′. Annealing of the RNA to DNA (1 RNA:3 DNAs) was performed in 50 mM Tris·HCl (pH 8.0), 80 mM KCl, and 1 mM DTT. Components were mixed, heated to 95°C, and slow-cooled to room temperature.

RNase H Assays. Reactions were performed as described by Palaniappan *et al.* (20). Samples were subjected to 10% denaturing PAGE and analyzed by a PhosphorImager (Molecular Dynamics) by using IMAGEQUANT version 1.2. Background band density in the zero time point was subtracted from the quantitation of each cleavage product to determine the rates. The rates were determined graphically by plotting concentration of product versus time by using linear regression. The rates were calculated and averaged from three independent experiments. An RNA ladder created by base hydrolysis determined the lengths of RNA products.

Quench-Flow Assay. Fast reactions were performed by using a Kin Tek Instruments (University Park, PA) quench-flow apparatus. A mixture containing 50 mM Tris·HCl (pH 8.0), 1 mM DTT, 1 mM EDTA, 34 mM KCl, 40 nM substrate, and 80 nM HIV-RT was injected into one sample line. The enzyme was allowed to prebind to the substrate for 2 min at 37°C and was immediately injected into the machine for reaction. A mixture containing 50 mM Tris·HCl (pH 8.0), 1 mM DTT, 1 mM EDTA, 34 mM KCl, and 12 mM $MgCl_2$ was injected into the other sample line. The reaction was mixed at approximately 30°C in one of the seven reaction loops, dependent on the time. The reactions were quenched with 2× termination mixture. The products were analyzed as described in the above section.

Results and Discussion

Several studies have shown that HIV-1 RT leaves behind RNA fragments while synthesizing DNA (7, 12, 18, 19, 26). We hypothesized that RT would bind and cleave these RNAs by the polymerase-independent mode of cleavage. We examined the specificity and the rates of each RNase H cut made by RT to determine the mechanism of this process.

A 41- or 50-nt RNA was annealed to a 77-nt DNA such that the RNA was recessed on the template. In previous studies, we found that RT makes a primary cut predominantly 18 nt in length from the 5′ end of recessed RNAs (20, 21). The enzyme also makes a secondary cut 8–9 nt from this 5′ end. Based on these findings, we initially proposed that RT cleaves RNA fragments by a stepwise mechanism of cuts: primary, secondary, next primary, then next secondary (Fig. 1). We believed the primary and secondary cuts would cleave the first 18 nt into fragments small enough to dissociate readily from the DNA template. This process would allow an RT to bind to the new 5′ end of the RNA to create the set of cuts. If this model were true, complete cleavage of the 41-nt RNA fragment would require two primary and two secondary cuts, whereas removal of the 50-nt RNA fragment would require one or more additional cuts.

Rates of the Primary and Secondary Cuts. To test this hypothesis, we first determined the rates of each type of cut. An excess of substrate compared with enzyme was used such that initial rates could be determined. Fig. 2*A* shows a time course experiment using the 5′ end labeled 41-nt RNA substrate. Two products appeared over time. The first was 15–19 nt in length, with a predominant product 18 nt in length, and the second was 8–9 nt in length. Several bands occur around each predominant cut, presumably because RT can slide transiently on the template. Fig. 2 shows the secondary product increasing linearly over time with a rate of 2.1×10^{-4}nM/sec (Fig. 2*C* and Table 1). The amount of the 18-nt product increased more rapidly than that of the 8-nt product at first, but the product did not accumulate linearly over time (Fig. 2*C*). This result occurred because the RT destroys the 18-nt product to make the 8-nt product. The overall outcome suggests that the primary cut occurs at a faster rate than the secondary cut does. However, because the primary product is being destroyed, the rate of its formation cannot be quantitated (Fig.2*C*). Similar results were obtained for the 5′ end-labeled 50-nt substrate (Fig. 2*B*). The rate for the secondary cut on this substrate was 2.4×10^{-4}nM/sec (Table 1).

To compare rates of the primary and secondary cuts in enzyme excess, reactions were performed in a Kin Tek quench-flow machine. Enzyme excess was used to produce sufficient band density for visualization of the cleavage products within the short

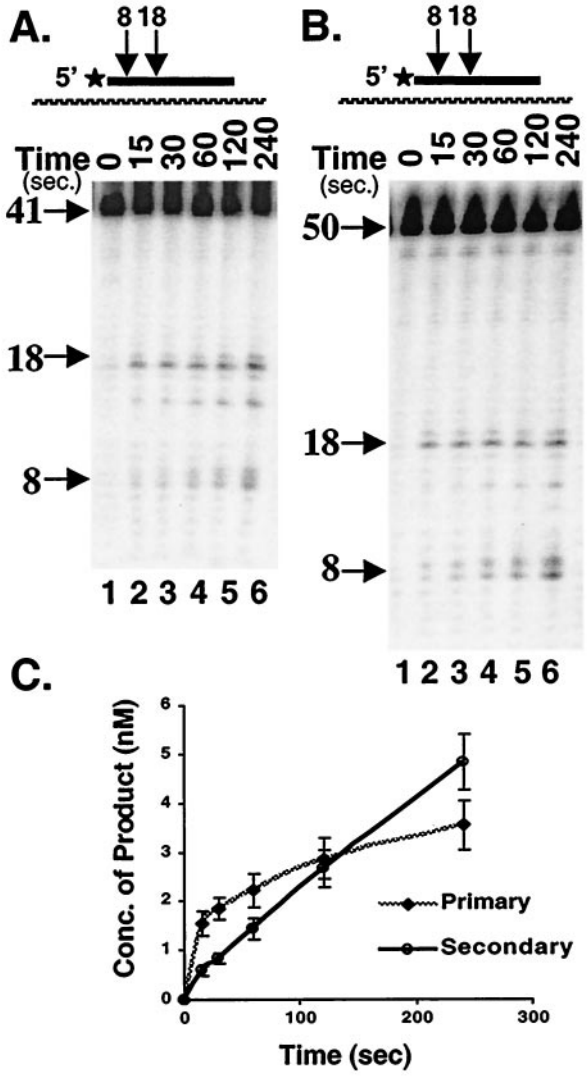

Fig. 2. An RNase H time course assay of the primary and secondary cuts using an excess of substrate to enzyme. (*A* and *B*) The time course experiment with the 5′ end-labeled 41- and 50-nt RNA substrates, respectively. Above each panel is a representation of the substrate. The length of each product is indicated by the numbered arrows. The star indicates the position of the ^{32}P label. Each experiment was performed with a ratio of 1 enzyme to 37 substrates. The time points are indicated above each lane. The numbered arrows indicate the lengths of the starting material and products, which were determined from an RNA ladder created by base hydrolysis. The 18- and 8-nt products correspond to the primary and secondary cuts. (*C*) A representative graph of the 41-nt RNA substrate and is plotted as concentration of product formed versus time.

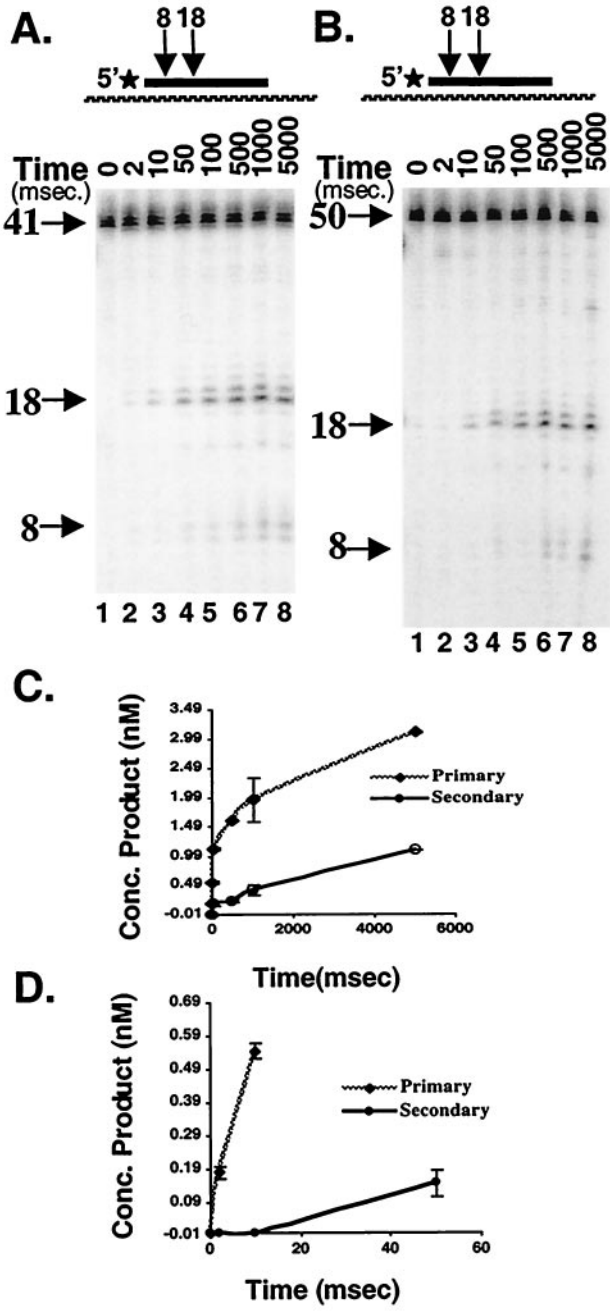

Fig. 3. An RNase H time course assay of the primary and secondary cuts using the quench-flow machine. (*A* and *B*) The time course with the 41- and 50-nt RNA, respectively. The substrates are represented above each panel. The experiments were performed with a 2 enzyme to 1 substrate ratio. The time points are in milliseconds and shown above each lane. (*C*) The graph of the 41-nt RNA substrate plotted as concentration of product formed (nM) versus time (msec). (*D*) The first three time points of the reaction. This plot shows the initial burst of the primary cut.

sampling times of the quench-flow apparatus. This approach differs from the previous experiment where substrate excess is used to prevent saturation of the cleavage reaction. The same 5′ end-labeled substrates were used as in the previous experiment. Because quench-flow can capture millisecond time points, the rate of a fast reaction can be accurately determined, even if much slower reactions are removing the product. Fig. 3 shows a time course with 5′ end-labeled 41- and 50-nt RNA substrates. The first product observed was that of the primary cut (Fig. 3*A*, lanes 2 and 3). Products of the secondary cut appeared at the 50-ms

Table 1. The initial rates of the secondary, second primary, and 5-nt cuts

RNA	Secondary	20-nt	Second primary	5-nt
41	2.1 ± 0.07	NA	NA	2.0 ± 0.50
50	2.4 ± 0.70	1.0 ± 0.14	1.8 ± 0.14	2.4 ± 0.60

NA, not applicable to the length of RNA. The units for the rates are $\times 10^{-3}$ nM/sec.

Table 2. The rates of the primary, secondary, and 5-nt cuts using the quench-flow machine

RNA	Primary: Burst, $\times 10^{-2}$	Primary: Steady-state, $\times 10^{-3}$	Secondary, $\times 10^{-4}$	5-nt, $\times 10^{-4}$
41	3.0 ± 0.01	1.7 ± 0.35	5.5 ± 0.70	5.6 ± 0.60
50	1.9 ± 0.01	2.4 ± 0.66	3.6 ± 0.57	2.0 ± 0.70

The units for the rates are nM/msec.

time point. This result shows that the primary cut occurs faster than the secondary cut does. The primary cut has two rates, a fast burst and a slower steady state (Fig. 3*C*). The burst rate of the primary cut was calculated from the first three time points and is 0.03 nM/ms and 0.019 nM/ms for the 41- and 50-nt RNA substrate, respectively (Fig. 3*D*). RTs prebound to the substrate in the exact position or conformation for reaction are the likely cause of the burst. RT would be able to cleave immediately when the $MgCl_2$ was added. The secondary cut did not have measurable burst kinetics (Fig. 3*D*).

In the steady-state period, both the primary and the secondary cuts occurred and their rates were compared (Fig. 3*C* and Table 2). The 41- and 50-nt RNA substrates showed similar trends. For the 41-nt RNA substrate, the primary and the secondary cuts occurred at rates of 1.7×10^{-3} nM/ms and 5.5×10^{-4} nM/ms, respectively. The primary cut was 3 times faster than the secondary cut was. For the 50-nt RNA, the primary and secondary rates were 2.4×10^{-3} nM/ms and 3.6×10^{-4} nM/ms, respectively, such that the primary cut was 6 times faster than the secondary cut was. Because the 50-nt RNA is longer than the 41-nt RNA, RT has more potential binding sites. The wider binding distribution results in a slower rate for the secondary cut than with the 41-nt RNA. The primary cut occurs at a high-affinity site, with no difference in rates between the two substrates. Hence, this observation is why the primary and secondary cuts differ by 3-fold on the shorter substrate and 6-fold on the longer substrate. Overall, these observations are consistent with a stepwise mechanism based on the relative rates of each cut.

The Second Primary and 5-nt Cut Rates. The stepwise mechanism predicts that the next primary cut would follow after the first secondary cut. To examine this premise, the 41- and 50-nt RNA substrates were 3′ end-labeled, and a conventional time course assay was performed in substrate excess. The experiment using the 41-nt RNA substrate showed products ranging from 22 to 24 nt in length with a predominant product 23 nt (Fig. 4*A*). This product represents the first primary cut. The less intense bands around the primary product apparently occur by transient RT sliding on the template. The rate of this cut could not be determined because this primary cleavage product is cut into smaller segments. If the second primary cut occurs, an RT would align to the new 5′ end generated by the previous primary cut. The resultant cleavage would create a product 5 nt in length from the 3′ end of the 41-nt RNA substrate. We observed products 5–7 nt in length that corresponded to this cut. The rate of formation of these products was 2.0×10^{-4} nM/sec, which was nearly identical to the secondary cut rate. Similar results were observed with the 50-nt RNA substrate. The predominant product, which was 32 nt in length, corresponded to the primary cut. A second primary cut was expected to make fragments approximately 14 nt in length. Products 10–17 nt in length, with the predominant length being 13 nt, were observed. The rate for this product group was 1.8×10^{-4} nM/sec (Table 1), which was similar to the rate for the corresponding cut on the 41-nt RNA substrate.

Another set of products, 20–22 nt in length, appeared over time from the 50-nt RNA. The rate for this product group was

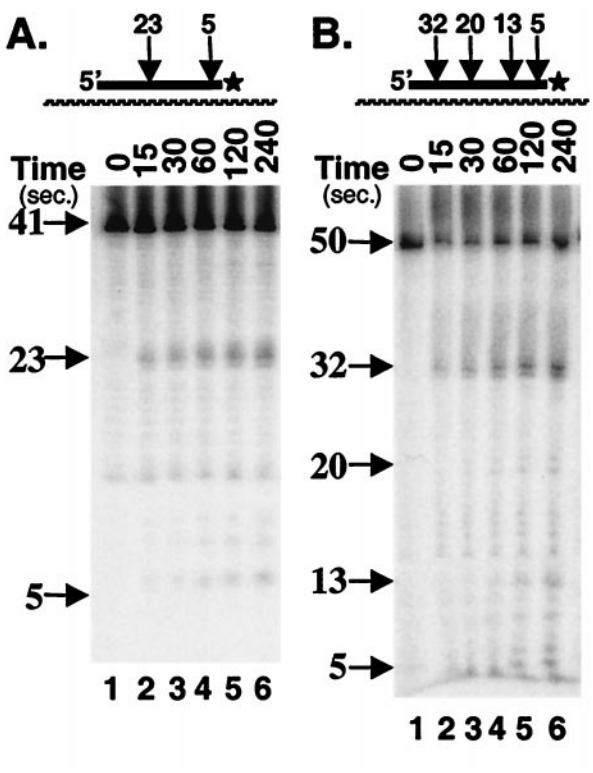

Fig. 4. A time course of the primary, second primary, and 5-nt cuts using an excess of substrate to enzyme ratio. The star at the 3′ end represents the ^{32}P label. As in the previous figures, the numbered arrows adjacent to the image indicate the length of the starting material and products. (*A*) The time course with the 41-nt substrate. The 23-nt product is the primary cut. The 5- to 7-nt products are the second primary or 5-nt cuts. (*B*) The experiment using the 50-nt RNA substrate. The 32-nt product represents the primary cut. The 20- to 22-nt and 17- to 13-nt products are the second primary cuts. The 5-nt band represents the 5-nt cut.

1.0×10^{-4} nM/sec, which is slightly slower than the secondary and second primary cuts. These products could arise from an enzyme aligned to the 5′ end of the RNA created by the secondary cut. Their rate is consistent with such an alignment, because they appear slightly slower than the necessary secondary cleavage. Another possibility is that there are internal cuts occurring independent of the 5′ end alignment.

The 50-nt RNA requires an additional cut to cleave the remaining 10- to 13-nt fragments. Interestingly, products 5–7 nt in length were made from the 3′ end-labeled 50-nt RNA. These products appeared at a rate of 2.4×10^{-4} nM/sec. We believe RT binds or slides to the 3′ end of the RNA. RT would then align its carboxyl terminus to this end, which places the RNase H active site in the correct position for the 5-nt cut (Fig. 6; refs. 23 and 27). This positioning is consistent with recent results mapping the binding site of the last carboxy α-helix of the RT (27). Rausch *et al.* (27) showed that this structure binds an additional 5 nt past the RNase H active site, causing the enzyme to span 23–24 nt of an RNA/DNA hybrid. This observation also means that the 5- to 7-nt products that we measured on the 41-nt RNA could have been created as a 5-nt cut, a second primary cut, or both (Fig. 6).

The similar rates of the second primary, secondary, and 5-nt cuts would seem to be consistent with a branch pathway in which the primary cut is first, followed by either a secondary, second primary, or 5-nt cut. However, the results still could be consistent with a stepwise mechanism, as follows. The primary cut would occur first. The secondary cut would occur next and at a

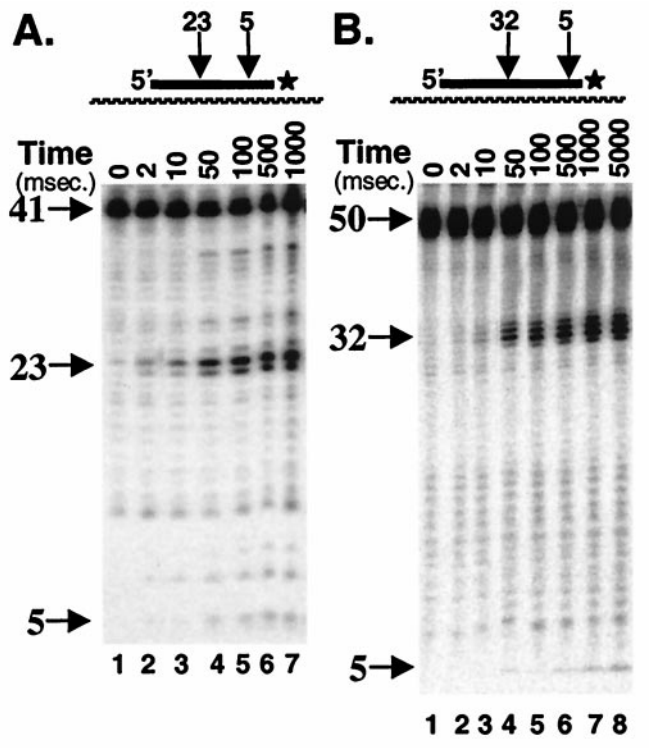

Fig. 5. A time course of the primary, second primary, and 5-nt cuts using the quench-flow machine. The same substrates were used as in Fig. 4. A ratio of 2 enzymes to 1 substrate was used. The time was measured in milliseconds and the time points are labeled above each lane. (*A*) The time course of the 3′ end-labeled 41-nt RNA. The 23-nt and 5-nt products are the primary and 5-nt cuts, respectively. (*B*) The time course with the 50-nt RNA substrate. The 32-nt and 5-nt products are the primary and 5-nt cuts.

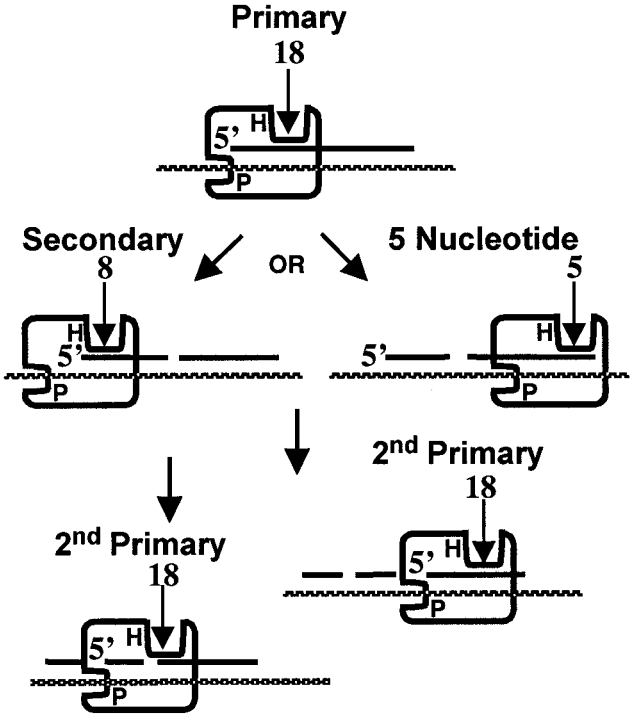

Fig. 6. The order of cleavages of an RNA fragment made by HIV-1 RT. The same symbols were used as in Fig. 1. The primary cut occurs first, followed by the secondary and 5-nt cuts. The second primary cuts are made last.

relatively slow rate. Then, if the second primary and 5-nt cuts were fast, all cuts after the primary would seem to have similar rates as that of the secondary cut. To distinguish between these two mechanisms, we used quench-flow to examine the rates of these cleavages in more detail. Measurement in the millisecond range allows more accurate calculation of the rates and determination of the order of events.

The RNA Cleavage Mechanism of HIV-1 RT. Fig. 5 shows the quench-flow time course of RNase H activity on the 3′ end-labeled 41- and 50-nt RNA substrates. Graphs of these time courses were similar to those of the 5′ end-labeled substrates in Fig. 3 (data not shown). Both substrates show the primary cut occurring within the 2-msec time point. As expected, the rates for this cut were identical to those observed with the 5′ end-labeled substrates (Table 2). With the 41-nt substrate, the next cleavage creates 5- to 7-nt fragments. This product could result from the second primary cut or the 5-nt cut. The rate for this cut was the same as that of the secondary cut, at 5.6×10^{-4} nM/msec. This result is consistent with the long time frame experiment and supports a branched mechanism. With the 50-nt RNA substrate, the rate of the 5-nt cut was 2.0×10^{-4} nM/msec. This cut was made at the same rate as the secondary cut on this substrate. The second primary cuts on the 50-nt RNA were not observed. The minor degradation products of the starting material, present before the reaction at a similar position as the 13- to 17-nt products, did not increase over time (Fig. 5*B*). Also the 20- to 22-nt products were not detected in this experiment. These results show that the second primary cut does not occur in this time frame. The latter products must arise at a slower rate than do the secondary and 5-nt cuts. These results would favor a modified branched mechanism in which the primary cut occurs first (Fig. 6). Then, the same enzyme or another enzyme would slide or bind to the secondary or 5-nt site and make the next cut. Finally, RT would create the second primary cuts until the RNA is removed.

Because RT uses the same active site for each cleavage event, the rates of each cut must depend on the relative affinity for binding and cleavage at various positions on the RNA. By this reasoning, RT would bind to the primary site with the highest affinity, and to the secondary and 5-nt positions with similar lower affinities. We believe that the RT binds first to the primary site, as suggested by the burst kinetics measured at this site after prebinding with RT. We hypothesize that RT can move in either direction from this site with equal probability to make other cuts. The second primary cut sites on the 50-nt RNA substrate seemed to be least susceptible to cleavage than the other positions were. Possibly, the RNA fragments created from the previous primary and secondary cuts do not dissociate from the template and may complicate the positioning of RT for the second primary cut. The ladder of products, ranging from 10 to 17 nt in length, suggests that the RT is tethered loosely at this site or can even position without measuring from a 5′ end.

In contrast to results with the 41-nt RNA, the second primary cut on the 50-nt RNA occurred after the first 5 sec of the reaction. This result would suggest that the 5- to 7-nt product of the 41-nt RNA mostly is derived from 3′ end positioning of the RT, rather than from being the product of a second primary cut. Previously, we showed that HIV-1 RT cleaves up to 80% of the RNA during primer elongation, with 20% of the RNA remaining as fragments ranging from 13 to 45 nt in length. Because the lengths of RNA fragments *in vivo* have not been determined, the second primary cut may be required less frequently for the cleavage of naturally occurring fragments. RT may use the

primary, secondary, and 5-nt cuts for the removal of the majority of RNA fragments.

Overall, this report shows that, for HIV-1 RT, the polymerase-independent RNase H activity can efficiently remove the RNA genome after DNA synthesis. Experiments performed in enzyme excess demonstrate that RNA is cleaved as early as 2 msec. Most RNA fragments are cleaved by a combination of primary, secondary, second primary, and 5-nt cuts within 1 min (data not shown).

The polymerase-independent mode of RNase H activity is also a key component of the minus strand transfer reaction. Virions containing RNase H-minus RT fail at the minus strand transfer step (6). When polymerase-deficient RT and an RNase H-minus RT were combined in a single viral particle, replication was restored, but at a slower rate (5). In this experiment, because the RT that synthesizes the DNA does not have RNase H activity, the RNA genome is cleaved by the polymerase-minus RT, indicating that polymerase-independent RNase H activity is sufficient for viral replication. *In vitro* studies examining minus strand transfer and RNase H activity at the 5′ end of the HIV genome have shown the accumulation of 8- to 15-nt products (14, 15, 26). The secondary cut on these fragments is very slow, showing that RT must require a 3′ overhang on the DNA template in order for the enzyme to move back to create this cut (Fig. 6). Without this 8-nt cut, the 3′ end of the DNA is not free to complete minus strand transfer. The presence of nucleocapsid protein enhances the rate of this cut significantly (28). Inhibitors of this cut also show inhibition of the minus strand transfer reaction (29). This result demonstrates the importance of the polymerase-independent secondary cleavage reaction to viability of the virus.

Importantly, this report determines the overall mechanism for the removal of RNA fragments. Understanding the polymerase-independent mode of RNA cleavage should aid in efforts to find different inhibitors against the RNase H activity. Most inhibitors of HIV-1 RT interfere with polymerization. Several compounds have been found to inhibit RT RNase H, but none have been used therapeutically yet. Illimaquinone and *N*-ethylmaleimide inhibit the RNase H catalysis of both HIV-1 and HIV-2 RT (30, 31). Both drugs seem to exert their effects near the 280-cysteine residue of RT. They are believed to alter the structure of RT to prevent RNase H activity. A recently described inhibitor, PD126338, seems to specifically inhibit the polymerase-independent mode of cleavage and to prevent minus strand transfer *in vitro* (29). In the presence of the drug, RNA fragments with lengths of 18 nt and larger accumulate over time. Based on our mechanism, we believe that this compound is inhibiting the secondary and 5-nt cuts. This work points out the usefulness of knowing the details of the RNase H cleavage mechanism.

This work was supported by the National Institutes of Health Grant GM 49573 and Core Grant CA 11198 to the University of Rochester Cancer Center. M.W. was supported by a fellowship from the National Institutes of Health Grant T32 DE 07207-09.

1. Barre-Sinoussi, F., Chermann, J. C., Rey, F., Nugeyre, M. T., Chamaret, S., Gruest, J., Dauguet, C., Axler-Blin, C., Vezinet-Brun, F., Rouzioux, C., *et al.* (1983) *Science* **220,** 868–871.
2. Brown, P. O. (1997) in *Retroviruses*, ed. Coffin, J. M., Hughes, S. H. & Varmus, H. E. (Cold Spring Harbor Lab. Press, Plainview, NY), 121–169.
3. Goff, S. P. (1990) *J. Acquired Immune Defic. Syndr.* **3,** 817–831.
4. Champoux, J. J. (1993) in *Reverse Transcriptase*, ed. Skalka, A. M. & Goff, S. P. (Cold Spring Harbor Lab. Press, Plainview, NY), pp. 103–117.
5. Telesnitsky, A. & Goff, S. P. (1993) *EMBO J.* **12,** 4433–4438.
6. Tanese, N., Telesnitsky, A. & Goff, S. P. (1991) *J. Virol.* **65,** 4387–4397.
7. Kelleher, C. D. & Champoux, J. J. (2000) *J. Biol. Chem.* **275,** 13061–13070.
8. Fuentes, G. M., Fay, P. J. & Bambara, R. A. (1996) *Nucleic Acids Res.* **24,** 1719–1726.
9. DeStefano, J. J., Buiser, R. G., Mallaber, L. M., Bambara, R. A. & Fay, P. J. (1991) *J. Biol. Chem.* **266,** 24295–24301.
10. Oyama, F., Kikuchi, R., Crouch, R. J. & Uchida, T. (1989) *J. Biol. Chem.* **264,** 18808–18817.
11. Wohrl, B. M., Volkmann, S. & Moelling, K. (1991) *J. Mol. Biol.* **220,** 801–818.
12. DeStefano, J. J., Mallaber, L. M., Fay, P. J. & Bambara, R. A. (1993) *Nucleic Acids Res.* **21,** 4330–4338.
13. Schultz, S. J., Zhang, M., Kelleher, C. D. & Champoux, J. J. (1999) *J. Biol. Chem.* **274,** 34547–34555.
14. Furfine, E. S. & Reardon, J. E. (1991) *J. Biol. Chem.* **266,** 406–412.
15. Peliska, J. A. & Benkovic, S. J. (1992) *Science* **258,** 1112–1118.
16. Post, K., Guo, J., Kalman, E., Uchida, T., Crouch, R. J. & Levin, J. G. (1993) *Biochemistry* **32,** 5508–5517.
17. DeStefano, J. J., Buiser, R. G., Mallaber, L. M., Myers, T. W., Bambara, R. A. & Fay, P. J. (1991) *J. Biol. Chem.* **266,** 7423–7431.
18. DeStefano, J. J., Mallaber, L. M., Fay, P. J. & Bambara, R. A. (1994) *Nucleic Acids Res.* **22,** 3793–3800.
19. Kati, W. M., Johnson, K. A., Jerva, L. F. & Anderson, K. S. (1992) *J. Biol. Chem.* **267,** 25988–25997.
20. Palaniappan, C., Fuentes, G. M., Rodriguez-Rodriguez, L., Fay, P. J. & Bambara, R. A. (1996) *J. Biol. Chem.* **271,** 2063–2070.
21. DeStefano, J. J., Bambara, R. A. & Fay, P. J. (1993) *Biochemistry* **32,** 6908–6915.
22. Kelleher, C. D. & Champoux, J. J. (1998) *J. Biol. Chem.* **273,** 9976–9986.
23. Gotte, M., Maier, G., Gross, H. J. & Heumann, H. (1998) *J. Biol. Chem.* **273,** 10139–10146.
24. Jacobo-Molina, A., Ding, J., Nanni, R. G., Clark, A. D., Jr., Lu, X., Tantillo, C., Williams, R. L., Kamer, G., Ferris, A. L., Clark, P., *et al.* (1993) *Proc. Natl. Acad. Sci. USA* **90,** 6320–6324.
25. Kohlstaedt, L. A., Wang, J., Friedman, J. M., Rice, P. A. & Steitz, T. A. (1992) *Science* **256,** 1783–1790.
26. Fu, T. B. & Taylor, J. (1992) *J. Virol.* **66,** 4271–4278.
27. Rausch, J. W., Sathyanarayana, B. K., Bona, M. K. & Le Grice, S. F. (2000) *J. Biol. Chem.* **275,** 16015–16022.
28. Peliska, J. A., Balasubramanian, S., Giedroc, D. P. & Benkovic, S. J. (1994) *Biochemistry* **33,** 13817–13823.
29. Gabbara, S., Davis, W. R., Hupe, L., Hupe, D. & Peliska, J. A. (1999) *Biochemistry* **38,** 13070–13076.
30. Loya, S. & Hizi, A. (1993) *J. Biol. Chem.* **268,** 9323–9328.
31. Loya, S., Gao, H. Q., Avidan, O., Boyer, P. L., Hughes, S. H. & Hizi, A. (1997) *J. Virol.* **71,** 5668–5672.